

# Source Chaoticity from Two- and Three-Pion Correlations in Au+Au collisions at $\sqrt{s_{\text{NN}}} = 130$ GeV

Kenji Morita,<sup>1,\*</sup> Shin Muroya,<sup>2,†</sup> and Hiroki Nakamura<sup>1,‡</sup>

<sup>1</sup>*Department of Physics, Waseda University, Tokyo 169-8555, Japan*

<sup>2</sup>*Tokuyama University, Shunan, Yamaguchi 745-8511, Japan*

(Dated: November 8, 2018)

We consistently analyze two-pion correlation functions and three-pion correlation functions of 130A GeV Au+Au collisions measured at RHIC, applying three models of partially coherent pion sources. The effect of long-lived resonances on the chaoticity in the two-pion correlation function is estimated on the basis of a statistical model. We find that the chaoticity extracted from the three-pion correlation function is consistent with that extracted from the two-pion correlation function at vanishing relative momenta after the subtraction of the contribution of the long-lived resonance decays. All three models indicate that pions are emitted from the mixture of a chaotic source and coherent sources in the 130A GeV Au+Au collisions.

PACS numbers: 25.75.Gz

## I. INTRODUCTION

Pion interferometry is one of the most powerful tools in relativistic heavy ion physics. The fact that two-boson intensity correlation functions provide information concerning the geometry of particle sources is known as the Hanbury Brown-Twiss (HBT) effect. The two-pion correlation function  $C_2(\mathbf{p}_1, \mathbf{p}_2)$  has been analyzed extensively to explore space-time structures of collision dynamics [1]. The HBT effect is based on the assumption of a chaotic source; i.e., particles are emitted with relatively random phases. The chaoticity index  $\lambda$  in the two-particle correlation function is defined as the two-pion correlation strength,  $\lambda = C_2(\mathbf{p}, \mathbf{p}) - 1$ . It is unity for a chaotic source and vanishes for a coherent one. Thermal emission is naturally regarded as a perfect chaotic source, [2, 3] but non-thermal components need not be perfectly chaotic. For example, if a disoriented chiral condensation (DCC) region is produced, this domain can decay into coherent pions. Therefore, the chaoticity index  $\lambda$  is an important parameter for understanding multiple particle production. However, experimental data are not so simply understood; even for a chaotic source, the chaoticity can be reduced by some other effects, such as long-lived resonances [4, 5, 6, 7, 8].

As an alternative tool to investigate particle sources, the three-particle correlation function has also been proposed [9, 10, 11, 12]. Regarding the chaoticity of the sources, the three-particle correlation is a more promising tool than the two-particle correlation, because long-lived resonances do not affect a normalized three-pion correlator (third order cumulant correlation function),

$$r_3(\mathbf{p}_1, \mathbf{p}_2, \mathbf{p}_3) = \frac{[C_3(\mathbf{p}_1, \mathbf{p}_2, \mathbf{p}_3) - 1] - [C_2(\mathbf{p}_1, \mathbf{p}_2) - 1] - [C_2(\mathbf{p}_2, \mathbf{p}_3) - 1] - [C_2(\mathbf{p}_3, \mathbf{p}_1) - 1]}{\sqrt{[C_2(\mathbf{p}_1, \mathbf{p}_2) - 1][C_2(\mathbf{p}_2, \mathbf{p}_3) - 1][C_2(\mathbf{p}_3, \mathbf{p}_1) - 1]}}. \quad (1)$$

Here,  $C_2(\mathbf{p}_1, \mathbf{p}_2)$  and  $C_3(\mathbf{p}_1, \mathbf{p}_2, \mathbf{p}_3)$  are the two- and three-pion correlation functions defined as

$$C_2(\mathbf{p}_1, \mathbf{p}_2) = \frac{W_2(\mathbf{p}_1, \mathbf{p}_2)}{W_1(\mathbf{p}_1)W_1(\mathbf{p}_2)}, \quad (2)$$

and

$$C_3(\mathbf{p}_1, \mathbf{p}_2, \mathbf{p}_3) = \frac{W_3(\mathbf{p}_1, \mathbf{p}_2, \mathbf{p}_3)}{W_1(\mathbf{p}_1)W_1(\mathbf{p}_2)W_1(\mathbf{p}_3)}, \quad (3)$$

with  $W_n(\mathbf{p}_1, \dots, \mathbf{p}_n)$  being the  $n$  particle distribution. The chaoticity index in the three-pion correlator is the weight factor  $\omega = r_3(\mathbf{p}, \mathbf{p}, \mathbf{p})/2$ , which becomes unity for a chaotic source. The three-pion correlator used in the current

\*Electronic address: morita@hep.phys.waseda.ac.jp

†Electronic address: muroya@yukawa.kyoto-u.ac.jp

‡Electronic address: naka@hep.phys.waseda.ac.jp

experiments is a modified form of Eq. (1), introduced due to a lack of statistics, as

$$r_3(Q_3) = \frac{[C_3(Q_3) - 1] - [C_2(Q_{12}) - 1] - [C_2(Q_{23}) - 1] - [C_2(Q_{31}) - 1]}{\sqrt{[C_2(Q_{12}) - 1][C_2(Q_{23}) - 1][C_2(Q_{31}) - 1]}}, \quad (4)$$

where  $Q_{ij} = \sqrt{-(p_i - p_j)^2}$  and  $Q_3 = \sqrt{Q_{12}^2 + Q_{23}^2 + Q_{31}^2}$ , and  $\omega$  is defined as  $r_3(0)/2$ . In both definitions,  $\omega$  is expected to approach the same value at small  $Q_3$ .

In this paper, we analyze both the three- and two-pion correlation data measured by the STAR collaboration [13] for central events in Au+Au collisions at 130A GeV using three kinds of partially coherent models. The STAR collaboration, adopting a partial coherent model for the pion source, concludes that about 80% of pions are emitted from a chaotic source in the central collision events, and the chaoticity depends on the centrality [13]. In Ref. [13], analysis is carried out only with the three-pion correlation function, because the two-pion correlation function suffers from the effect of long-lived resonance decays. Hence, the chaoticity extracted from the three-pion correlation differs from that measured as the strength of the two-pion correlation function. One of the aims of this work is to account for this discrepancy. After an appropriate correction for the long-lived resonance decay contribution to the two-pion correlation function, the “true” chaoticity of the two-pion correlation function thereby obtained should be consistent with that extracted from the three-particle correlation function. We show that the chaotic fraction and the number of coherent sources evaluated from the “true” chaoticity of the two-pion correlation function are consistent with those obtained from the three-pion correlation function. Then, we study the structure of the source using three kinds of partial coherent source models. This paper is organized as follows. We give a brief explanation of the three kinds of source models in the next section. In Sec. III, we make corrections to the two-pion correlation for the long-lived resonance decay contributions. Section IV is devoted to a combined analysis of two- and three-pion correlation functions and analyses using the three models.

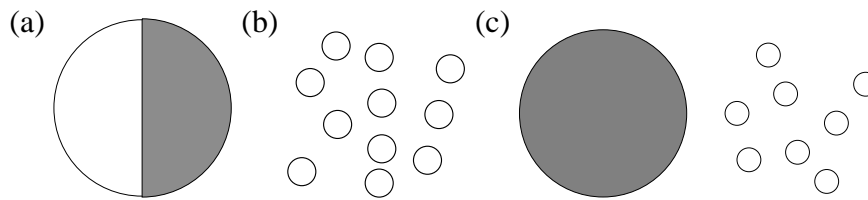


FIG. 1: Schematic depiction of Model I-III. The shaded areas represent the chaotic sources. The open area and small circles represent the coherent sources. (a) Model I, (b) Model II, (c) Model III.

## II. MODELS OF PION EMISSION

Let us start by giving a brief explanation of the models. In Model I, a chaotic source and a coherent source are assumed to be produced in every event of the collisions. This is a very limited case, because, in general, more than one coherent source can be produced in a collision. In Model II, we consider the case in which multiple coherent sources are produced. Model III is a mixture of Models I and II. A schematic depiction of the models is given in Fig. 1.

Model I is a partially coherent model [10] in which the solitary parameter  $\varepsilon_{pc}$  represents the ratio of the particle number emitted from the chaotic source to that emitted from both sources. In this model, pions are emitted from a mixture of a chaotic (thermal) and a coherent source. Here we do not discuss the origin of the coherent component. In general, we need to fix the source function of the coherent component, as well as that of the chaotic one, in order to express the correlation functions. Fortunately, because the chaoticity  $\lambda$  and the weight factor  $\omega$  are given by the correlation functions at vanishing relative momenta, they can be expressed in terms of the chaotic fraction as

$$\lambda = \varepsilon_{pc}(2 - \varepsilon_{pc}), \quad \omega = \sqrt{\varepsilon_{pc}} \frac{3 - 2\varepsilon_{pc}}{(2 - \varepsilon_{pc})^{3/2}}. \quad (5)$$

Model II is a multicoherent source model, [12] in which the source is composed of a large number of similar, independent coherent sources. Here we do not discuss the origin of the coherence. Because each small coherent source is independent, a chaotic source is realized as a cluster of an infinite number of the coherent sources. Here,  $\lambda$  and  $\omega$  are given by

$$\lambda = \frac{\alpha_m}{\alpha_m + 1}, \quad \omega = \frac{1}{2} \frac{2\alpha_m^2 + 2\alpha_m + 3}{\alpha_m^2 + 3\alpha_m + 1} \sqrt{\frac{\alpha_m + 1}{\alpha_m}}, \quad (6)$$

where  $\alpha_m$  represents the mean number of coherent sources, which obeys the Poisson distribution. Note that each of the above two models contains only a single parameter ( $\varepsilon_{\text{pc}}$  for Model I and  $\alpha_m$  for Model II) for two quantities, the chaoticity  $\lambda$  and the weight factor  $\omega$ . Model III is a mixture of these two [12] [see also Fig. 1(c)] and has already been applied to the SPS data by one of the present authors (H. N.). [14] This model contains two parameters, which are related to  $\lambda$  and  $\omega$  as

$$\lambda = \frac{\alpha}{\alpha + (1 - \varepsilon)^2}, \quad (7)$$

$$\omega = \frac{2\alpha^2 + 2\alpha(1 - \varepsilon)^2 + 3(1 - \varepsilon)^3(1 - 2\varepsilon)}{2[\alpha^2 + 3\alpha(1 - \varepsilon)^2 + (1 - \varepsilon)^3]} \sqrt{\frac{\alpha + (1 - \varepsilon)^2}{\alpha}}, \quad (8)$$

where  $\varepsilon$  and  $\alpha$  are the ratio of the number of particles from the chaotic source to the total number and the mean number of coherent sources, respectively.

Substituting  $\lambda$  and  $\omega$  from the experimental data into the above equations, we can obtain the parameters of the models,  $\varepsilon$  and  $\alpha$ . In Models I and II,  $\lambda$  and  $\omega$  must provide consistent values for the single parameter  $\varepsilon_{\text{pc}}$  or  $\alpha_m$ . As noted in the previous section, the STAR group analysis of the weight factor  $\omega$  in the central Au+Au collisions at  $\sqrt{s_{NN}} = 130$  GeV based on Model I indicates a value of  $\varepsilon_{\text{pc}} \simeq 0.8$ , which corresponds to  $\lambda \simeq 0.94$  [13]. Such a large  $\lambda$  seems to contradict the two-particle correlation data. However, we make a correction for the long-lived resonances in the two-pion correlation function before proceeding to conclusive calculations to obtain the parameters  $\varepsilon$  and  $\alpha$  using Eqs. (5)–(8). Then we show that the analysis of STAR is consistent with the value of  $\varepsilon^{\text{pc}}$  obtained from the resonance-corrected chaoticity.

### III. LONG-LIVED RESONANCE DECAY CONTRIBUTIONS TO $\lambda$

The existence of long-lived resonances that decay into pions causes the apparent reduction of the chaoticity in the two-pion correlation function. This is because the pion source caused by the long-lived resonance decay spreads over a much larger scale than that which is measurable with the present experimental resolution. The reduction factor  $\lambda^{\text{eff}}$  is related to the fraction of pions from long-lived resonances as [6]

$$\sqrt{\lambda^{\text{eff}}} = 1 - \frac{N_{\pi}^{\text{r}}}{N_{\pi}}, \quad (9)$$

with  $N_{\pi}$  being the total number of emitted pions and  $N_{\pi}^{\text{r}}$  being the number of pions emitted from long-lived resonances. We estimate the fraction of the  $\pi^{-}$  originating from the resonances with the help of a statistical model. According to the recent analyses, this statistical model provides a simple and good description of the particle yields of the RHIC experiments [15, 16]. We take account of the resonances up to  $\Sigma^{*}(1385)$ , in accordance with Ref. [8]. We treat  $K_s^0, \eta, \eta', \phi, \Lambda, \Sigma$  and  $\Xi$  as the long-lived resonances whose widths are smaller than 5 MeV. Heavier resonances can be ignored, because their contributions are thermally suppressed. The thermodynamic parameters are determined with a  $\chi^2$  fitting to the experimental data for the particle ratio. Here we take into account  $\bar{p}/p, \bar{p}/\pi^{-}, K^{-}/\pi^{-}, K^{*0}/h^{-}, K^{*0}/K^{*0}, \bar{\Lambda}/\Lambda$  and  $\bar{\Xi}/\Xi$ . From the fit, we obtain the temperature  $T = 158 \pm 9$  MeV and the chemical potential with respect to the baryon number  $\mu_{\text{B}} = 36 \pm 6$  MeV, with  $\chi^2/\text{dof} = 2.4/5$  [17]. For simplicity, we fix the chemical potential with respect to the third component of the isospin as  $\mu_{I_3} = 0$ . This does not affect the result, because the experimental data show  $\pi^{-}/\pi^{+} \simeq 1$ . The ratio of the number of particles  $i$  to the number of particles  $j$  can be calculated using the number densities in the local rest frame [18].

Then, the true chaoticity  $\lambda^{\text{true}}$ , which is characterized by the partial coherence of the source, is estimated as  $\lambda^{\text{true}} = \lambda^{\text{exp}}/\lambda^{\text{eff}}$ , with use of Eq. (9). In general,  $\lambda^{\text{exp}}$  obtained from the 1-dimensional Gaussian fitting can differ from that extracted from the 3-dimensional Gaussian fitting because of the projection, experimental resolution, and other effects, though these should be the same for an ideal measurement. In this paper, we use the value extracted from the 3-dimensional Gaussian fitting

$$C_2^{\text{fit}}(\mathbf{q}) = 1 + \lambda^{\text{exp}} \exp(-R_{\text{side}}^2 q_{\text{side}}^2 - R_{\text{out}}^2 q_{\text{out}}^2 - R_{\text{long}}^2 q_{\text{long}}^2), \quad (10)$$

as  $\lambda^{\text{exp}}$ . The STAR collaboration measured [19]  $\lambda^{\text{exp}}$  for three transverse momentum bins. Because the transverse momentum dependence of  $\lambda^{\text{exp}}$  agrees with the results obtained from Eq. (9) [8],  $\lambda^{\text{exp}}$  for the entire momentum range can be obtained by computing an average of  $\lambda_i^{\text{exp}}$  in which the square of the number of pions is used as the weight:

$$\bar{\lambda}^{\text{exp}} = \frac{\sum_{i=1}^3 \lambda_i^{\text{exp}} \int_{i\text{-th bin}} k_t dk_t (dN/k_t dk_t)^2}{\sum_{i=1}^3 \int_{i\text{-th bin}} k_t dk_t (dN/k_t dk_t)^2}. \quad (11)$$

Here,  $\lambda_i^{\text{exp}}$  and  $dN/k_t dk_t$  denote the measured chaoticity in the  $i$ -th bin and the pion transverse momentum distributions, respectively. We give a derivation of Eq. (11) in the appendix. In the calculation of Eq. (11), we use a result of the Bose-Einstein fit to the pion spectra carried out by the STAR collaboration [20].

Using Eq. (11), we find  $\bar{\lambda}^{\text{exp}} = 0.57 \pm 0.06$ .

Combining  $\lambda^{\text{eff}}$  obtained from the statistical model calculation, we finally obtain  $\lambda^{\text{true}} = 0.93 \pm 0.08$  for the present parameter region. The uncertainty of 0.08 is the sum of the experimental uncertainty on  $\bar{\lambda}^{\text{exp}}$  calculated from uncertainties on each  $\lambda_i^{\text{exp}}$  and  $dN/k_t dk_t$  and the statistical error propagated from the fit of the thermodynamic quantities  $T$  and  $\mu_B$  at  $1\text{-}\sigma$  confidence level.

#### IV. COMBINED ANALYSIS OF THE TWO- AND THREE-PARTICLE CORRELATION FUNCTION

In order to obtain the weight factor  $\omega$ , we have to extrapolate  $r_3(Q_3)$  [Eq. (4)] to  $Q_3 = 0$ . Because  $r_3(Q_3)$  is constructed from  $C_2(Q_{ij}) - 1$  and  $C_3(Q_3) - 1$  [Eq. (4)], we need to establish the functional forms of  $C_2(Q_{ij})$  and  $C_3(Q_3)$  so as to reproduce the experimental data (Figs. 2 and 3). Although quadratic and quartic fits to  $r_3(Q_3)$  at low  $Q_3$  are used in Ref. [13], we adopt an alternative approach, because the power law fits are relevant only for small  $Q_3$ , and it should be better to extrapolate  $r_3(Q_3)$  to  $Q_3 = 0$  after the fits of  $C_2$  and  $C_3$  within finite but broad relative momentum ranges. We also note that the  $Q_3$  dependence of  $r_3$  may be more complicated, [11] and the quadratic and quartic fitting tends to lead to an overestimated weight factor. In the following, we treat a set of  $\pi^-$  data measured in the lowest momentum bin for the event with the highest multiplicity.[13] We construct  $C_2$  and  $C_3$  from simple source functions with a set of parameters. This construction is determined by minimizing  $\chi^2$  with respect to the experimental data. For simplicity, we used a spherically symmetric Fourier-transformed source function with simultaneous emission,  $F_{ij} = f_{ij}(|\mathbf{q}_{ij}|)e^{i(E_i - E_j)t_0}$ , where the exponential term corresponds to emissions at a fixed time  $t_0$ . We believe that the assumption of instantaneous emission is a good approximation, because recent two-particle correlation data reveal a small time duration (*i.e.*  $R_{\text{out}} \sim R_{\text{side}}$ ). In addition, the existence of a finite time duration would not affect the following treatment, because it does not influence the chaoticity in the two-particle correlation function but, rather, decreases the width of the correlation function. For the spatial part,  $f_{ij}$ , we consider a Gaussian, an exponential, and a function written in terms of cosh, which becomes quadratic at small  $|\mathbf{q}|$  and exponential at large  $|\mathbf{q}|$ :

$$f_{1,ij}(|\mathbf{q}_{ij}|) = \exp(-R^2|\mathbf{q}_{ij}|^2/2), \quad (12)$$

$$f_{2,ij}(|\mathbf{q}_{ij}|) = \exp(-R|\mathbf{q}_{ij}|/2), \quad (13)$$

$$f_{3,ij}(|\mathbf{q}_{ij}|) = \frac{1}{\sqrt{\cosh(R|\mathbf{q}_{ij}|)}}. \quad (14)$$

Here,  $\mathbf{q}_{ij} = \mathbf{p}_i - \mathbf{p}_j$ , and  $R$  is the size parameter. The correlation functions are then calculated from the relations

$$C_2(\mathbf{p}_1, \mathbf{p}_2) = 1 + \lambda_{\text{inv}} \frac{f_{12}^2}{f_{11}f_{22}} \quad (15)$$

and

$$C_3(\mathbf{p}_1, \mathbf{p}_2, \mathbf{p}_3) = 1 + \nu \left( \sum_{(i,j)} \frac{f_{ij}^2}{f_{ii}f_{jj}} + 2\nu_3 \frac{f_{12}f_{23}f_{31}}{f_{11}f_{22}f_{33}} \right), \quad (16)$$

where  $\lambda_{\text{inv}}$ ,  $\nu$  and  $\nu_3$  are phenomenological adjustable parameters accounting for non-trivial coherence effects, and  $\sum_{(i,j)}$  is a summation over  $(i,j) = (1,2), (2,3), (3,1)$ . The forms Eqs. (15) and (16) are chosen so as to represent the chaotic case for  $\lambda_{\text{inv}} = 1$ ,  $\nu = 1$  and  $\nu_3 = 1$ . Equation (15) is a standard correlation function to fit data [19]. Although an alternative form of the three-particle correlation function,  $C_3 = 1 + \nu \sum_{(i,j)} \frac{f_{ij}^2}{f_{ii}f_{jj}} + 2\nu^{3/2} \frac{f_{12}f_{23}f_{31}}{f_{11}f_{22}f_{33}}$ ,<sup>1</sup> is often used, this equation corresponds to a perfectly chaotic source with a long-lived resonance decay contribution, and is incapable of taking into account non-trivial coherence effects. Therefore, we simply parametrize the three-particle correlation function by including the parameters from both the two-particle correlation part [the second term in Eq. (16)] and the genuine three-particle correlation part [the third term in Eq. (16)]. Note that we need only  $C_2(0) - 1$  and  $C_3(0) - 1$  to

---

<sup>1</sup> Actually, the resultant  $\chi^2$  value for this expression is worse than that for Eq. (16).

obtain  $\omega$ . We can set  $\nu_3 = 1$  without loss of generality for a description of  $C_3(Q_3)$  at small  $Q_3$ . Then, the parameters  $R$ ,  $\lambda_{\text{inv}}$  and  $\nu$  are determined through a simultaneous  $\chi^2$  fitting to both  $C_2(Q_{12})$  and  $C_3(Q_3)$ .

The three-particle correlator  $r_3(Q_3)/2$  is then obtained from separate projections of the numerator and denominator of Eq. (4) onto the single variable  $Q_3$  [21]. The results are depicted in Figs. 2–4 and listed in Table I.

TABLE I: Results of the  $\chi^2$  fitting to  $C_2$  and  $C_3$

$f( q )$	$R$ [fm]	$\lambda$	$\nu$	$\chi^2/\text{dof}$	$\omega$
$f_1$	$7.0 \pm 0.07$	$0.54 \pm 0.01$	$0.48 \pm 0.01$	110/30	$0.958 \pm 0.09$
$f_2$	$14.4 \pm 0.2$	$1.18 \pm 0.03$	$1.08 \pm 0.03$	79.7/30	$0.736 \pm 0.09$
$f_3$	$15.2 \pm 0.2$	$0.71 \pm 0.01$	$0.64 \pm 0.02$	15.8/30	$0.872 \pm 0.097$

The results show the failure of the Gaussian [Eq. (12)] and exponential [Eq. (13)] fittings. In Figs 2 and 3, each curve looks in agreement with the data, but the values of  $\chi^2/\text{dof}$  are larger than in the cosh source function case. Furthermore, the disagreement in  $r_3(Q_3)$  for the exponential (Gaussian) case reveals an over-estimation (under-estimation) of  $C_2$  in the extrapolation to small  $Q_{\text{inv}}$ . Constrastingly, the cosh source function [Eq. (14)] yields excellent agreement with the experimental data. Note that the resultant errorbars of  $\pm 0.097$  for  $\omega$  in the cosh case can also be obtained by an extrapolation of the error band expressed by the dash-dotted curves in Fig. 4. The error band is calculated using the propagation law from the errors of  $R$ ,  $\lambda_{\text{inv}}$  and  $\nu$  in the  $\chi^2$  fit ( $1-\sigma$  confidence level). Hence, our result for  $r_3$  in the cosh case is consistent with all the experimental data points, within the error bars.

The deviation in Fig. 4 for larger  $Q_3^2$  is not significant. Because both the numerator and denominator in Eq. (4) go to zero at the region, the projection requires a careful treatment and is strongly affected by unimportant tails. However, we do not know the *real* three-particle distribution which should be used as a weight. Therefore we use Eq. (16) instead. We confirmed that the most important quantity,  $\omega = r_3(0)/2$ , does not depend on the choice of the weight.

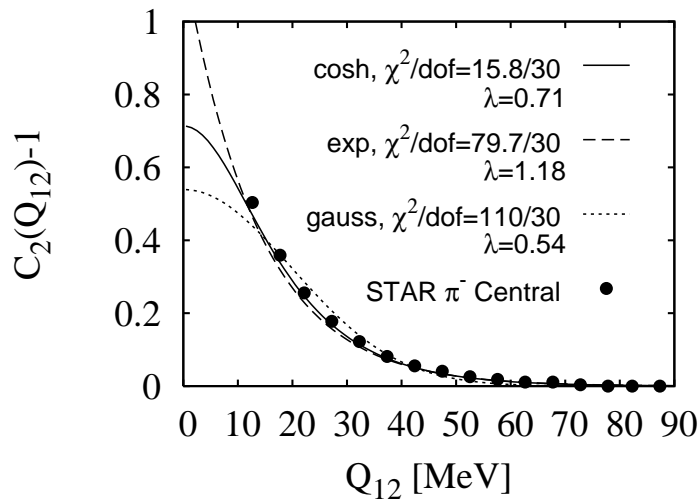


FIG. 2: Two-pion correlation function  $C_2(Q_{12})$ . The curves represent the results of the fits for each source function. The dots represent the experimental results taken from Ref. [19].

Now let us evaluate how chaotic the pion sources are by applying the models [Eqs. (5)–(8)] to the obtained values  $\lambda^{\text{true}} = 0.93 \pm 0.08$  and  $\omega = 0.872 \pm 0.097$ , where we adopt the result of the cosh source function. The allowed parameter regions of Models I and II are summarized in Table II. In these single-parameter models,  $\epsilon_{\text{pc}}$  and  $\alpha_{\text{m}}$  should give consistent results for the two input quantities,  $\lambda^{\text{true}}$  and  $\omega$ . Table II reveals that, after the appropriate correction for the long-lived resonance decay contributions to the two-pion correlation chaoticity index, the two-pion correlation function gives results consistent with the three-pion correlation function. The value of  $\epsilon_{\text{pc}}$  obtained from  $\omega$  is slightly smaller than that obtained in the previous analysis carried out by the STAR collaboration [13], while the values of  $\epsilon_{\text{pc}}$  obtained from  $\lambda^{\text{true}}$  and  $\omega$  are consistent with the result given in Ref. [13]. The very large uncertainty on

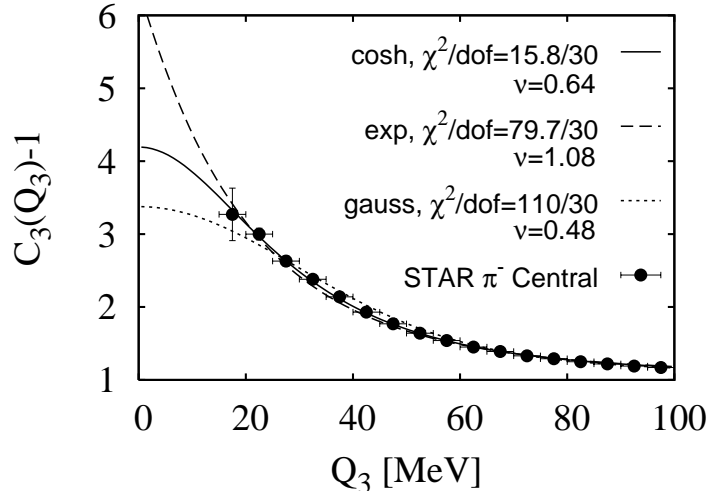


FIG. 3: Three-pion correlation function  $C_3(Q_3)$ . Here, the curves and dots have the same identifications as in Fig. 2. The experimental data are taken from Ref. [13].

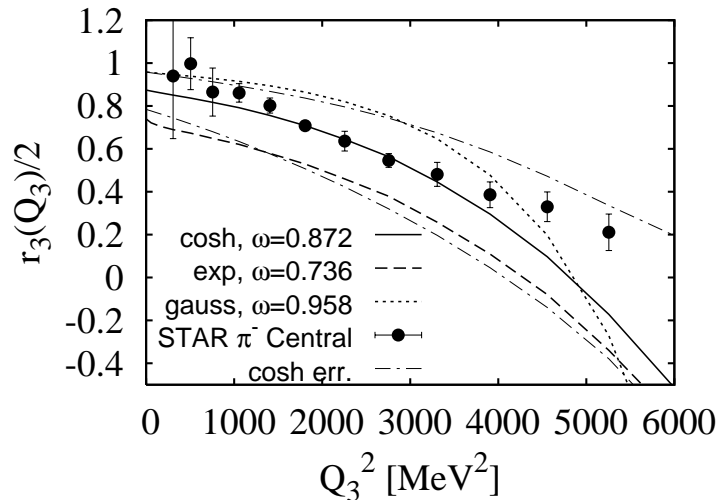


FIG. 4: The  $Q_3$  dependence of  $r_3/2$ . The curves and dots have the same identifications as in Figs. 2 and 3, except for the dash-dotted curves, which represent the upper and lower bounds of the cosh case. The experimental data are taken from Ref. [13]. See the text for details.

$\alpha_m$  is due to rapid changes of  $\alpha_m$  as a function of  $\lambda^{\text{true}}$  and  $\omega$  in these parameter regions. This feature may suggest the existence of a chaotic background introduced in Models I and III.

The success of extracting the “true” chaoticity by considering the long-lived resonance decay contribution suggests that it is needed to determine the source of pions, i.e., direct and short-lived resonance decay or long-lived resonance decay. Recently, a “partial” Coulomb correction has been proposed [22, 23] and actual computations have been carried out [24, 25], in which pions from long-lived resonance decays are treated separately. Such a correction affects not only the HBT radii but also  $\lambda^{\text{exp}}$ . We leave its treatment for future publications [26].

The allowed region of  $\varepsilon$  and  $\alpha$  for Model III is displayed in Fig. 5. In this figure, the darkest shaded area, labeled “III”, where the two lighter areas overlap, represents the ranges of  $\varepsilon$  and  $\alpha$  that correspond to the regions of  $\lambda_{\text{true}}$  and  $\omega$  estimated from the experimental data. The best fit point,  $\varepsilon = 0.75$  and  $\alpha = 0.77$ , is indicated by the solid square. Unfortunately, the uncertainty is still too large to provide strong constraints on the pion production mechanism. Nevertheless, the result shows a strong correlation between  $\alpha$  and  $\varepsilon$ ; that is, the experimental data reveal a mostly chaotic source which allows both a “partially coherent” picture ( $\alpha \sim 0, \varepsilon \leq 1$ ) and a “multicoherent” picture

TABLE II: Results for Models I and II

	Model I	Model II
From $\lambda$	$\varepsilon_{\text{pc}} = 0.73 \pm 0.14$	$\alpha_{\text{m}} = 12.6 \pm 14$
From $\omega$	$\varepsilon_{\text{pc}} = 0.65 \pm 0.11$	$\alpha_{\text{m}} = 7.6 \pm 9.7$

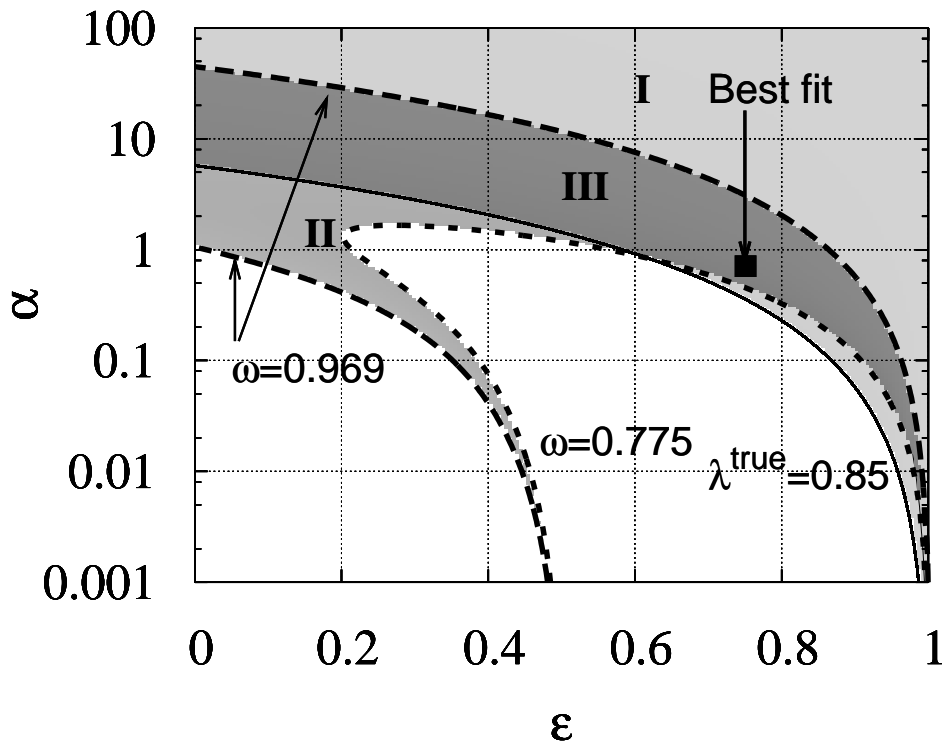


FIG. 5: Results for Model III. Area I is the allowed parameter region corresponding to the value of  $\lambda^{\text{true}}$  indicated by the solid line ( $\lambda^{\text{true}} = 0.85$ ). Area II, which is bounded by the dashed curve (upper bound of  $\omega$ ) and dotted curve (lower bound of  $\omega$ ), is the allowed parameter region corresponding to the range of  $\omega$ . Area III, which is characterized by overlap of areas I and II, is the allowed parameter region for  $\alpha$  and  $\varepsilon$ . The filled solid represents the best fit point.

( $\alpha \gg 1, \varepsilon \sim 0$ ). Though a fully chaotic source,  $\varepsilon = 1$ , is not excluded, the strong  $Q_3$  dependence of  $r_3(Q_3)$  seen in Fig. 4 is inconsistent with chaotic and symmetric sources. Even if the source is perfectly chaotic, the asymmetry of the source could cause a strong  $Q_3$  dependence. In this case, however,  $r_3$  becomes almost unity at small  $Q_3$ , while it deviates from unity at large  $Q_3$  [11]. Hence, we can claim that small coherent components are more likely to be produced.

In summary, we have given analyses of the two- and three-pion correlation data obtained by STAR, in terms of three kinds of partially coherent source models. We found that all three models give consistent description for both the three- and two-pion correlations if we take account of the apparent reduction of the chaoticity in the two-pion correlation function caused by the long-lived resonance decays. All models give the consistent picture that pion emission in the RHIC experiment is mostly chaotic, while coherent components are likely to exist (see Table II and Fig. 5). Further interesting problems concerning the multiplicity and the collision energy dependence of the chaoticity

will be published elsewhere [26].

### Acknowledgments

The authors would like to acknowledge Professor I. Ohba and Professor H. Nakazato for their support of this work. This work is partially supported by the Ministry of Education, Culture, Sports, Science and Technology, Japan (Grant No. 13135221) and Waseda University Grant for Special Research Projects (Nos. 2003A-095 and 2003A-591).

### APPENDIX A: DERIVATION OF $\bar{\lambda}^{\text{exp}}$

From Eq. (9), assuming that the  $k_t$  dependence of  $\lambda^{\text{exp}}$  is governed by the long-lived resonance decay contributions, we can write down  $\lambda_i^{\text{exp}}$  for midrapidity as

$$\lambda_i^{\text{exp}} = \frac{\int_{k_{t_{\min}}^i}^{k_{t_{\max}}^i} k_t dk_t \left( \frac{dN_{\text{dir+short}}}{k_t dk_t} \right)^2}{\int_{k_{t_{\min}}^i}^{k_{t_{\max}}^i} k_t dk_t \left( \frac{dN_{\text{total}}}{k_t dk_t} \right)^2}, \quad (\text{A1})$$

where  $N_{\text{dir+short}}$  and  $N_{\text{total}}$  represent the sum of the number of particles from direct emission and decay of short lived resonances and the total number of emitted particles, respectively. The values  $k_{t_{\min}}^i$  and  $k_{t_{\max}}^i$  are the minimum and maximum for a given momentum window of the  $i$ -th bin. Hence,  $k_{t_{\min}}^i = k_{t_{\max}}^{i-1}$ . Then, the domain of integration for the momentum acceptance,  $k_{t_{\min}} \equiv k_{t_{\min}}^1 < k_t < k_{t_{\max}}^n \equiv k_{t_{\max}}$ , with  $n$  being the number of the momentum bin, can be divided as

$$\int_{k_{t_{\min}}}^{k_{t_{\max}}} = \sum_{i=1}^n \int_{k_{t_{\min}}^i}^{k_{t_{\max}}^i}. \quad (\text{A2})$$

In terms of the above relation,  $\bar{\lambda}^{\text{exp}}$  can be written as

$$\bar{\lambda}^{\text{exp}} = \frac{\sum_{i=1}^n \int_{k_{t_{\min}}^i}^{k_{t_{\max}}^i} k_t dk_t \left( \frac{dN_{\text{dir+short}}}{k_t dk_t} \right)^2}{\sum_{i=1}^n \int_{k_{t_{\min}}^i}^{k_{t_{\max}}^i} k_t dk_t \left( \frac{dN_{\text{total}}}{k_t dk_t} \right)^2}. \quad (\text{A3})$$

Substituting Eq. (A1) into Eq. (A3), we obtain Eq. (11).

- 
- [1] B. Tomášik and U. A. Wiedemann, hep-ph/0210250.
  - [2] Y. Hama and S. S. Padula, Phys. Rev. D **37**, 3237 (1988).
  - [3] K. Morita, S. Muroya, H. Nakamura and C. Nonaka, Phys. Rev. C **61**, 034904 (2000).
  - [4] M. Gyulassy and S. S. Padula, Phys. Lett. B **217**, 181 (1988).
  - [5] J. Bolz, U. Ornik, M. Plümer, B. R. Schlei and R. M. Weiner, Phys. Rev. D **47**, 3860 (1993).
  - [6] T. Csörgő, B. Lörstad and J. Zimányi, Z. Phys. C **71** 491, (1996).
  - [7] H. Heiselberg, Phys. Lett. **379**, 27 (1996).
  - [8] U. A. Wiedemann and U. Heinz, Phys. Rev. C **56**, 3265 (1997).
  - [9] M. Biyajima, A. Bartl, T. Mizoguchi, N. Suzuki and O. Terazawa, Prog. Theor. Phys. **84**, 931 (1990).
  - [10] U. Heinz and Q. H. Zhang, Phys. Rev. C **56**, 426 (1997).
  - [11] H. Nakamura and R. Seki, Phys. Rev. C **60**, 064904 (1999).
  - [12] H. Nakamura and R. Seki, Phys. Rev. C **61**, 054905 (2000).
  - [13] J. Adams *et al.* (STAR Collaboration), Phys. Rev. Lett. **91**, 262301 (2003).
  - [14] H. Nakamura and R. Seki, Phys. Rev. C **66**, 027901 (2002).
  - [15] P. Braun-Munzinger, D. Magestro, K. Redlich and J. Stachel, Phys. Lett. B **518**, 41 (2001).
  - [16] W. Broniowski and W. Florkowski, Phys. Rev. Lett. **87**, 272302 (2001).
  - [17] The slightly smaller  $\mu_B$  than previous analyses comes from larger  $\bar{p}/p$  value in the revised experimental data, C. Adler *et al.* (STAR Collaboration), Phys. Rev. Lett. **90**, 119903(E) (2003).



- [18] J. Cleymans and K. Redlich, Phys. Rev. **C60**, 054908 (1999).
- [19] C. Adler *et al.* (STAR Collaboration), Phys. Rev. Lett. **87**, 082301 (2001).
- [20] J. Adams *et al.* (STAR Collaboration), nucl-ex/0311017.
- [21] M. M. Aggarwal *et al.* (WA98 Collaboration), Phys. Rev. Lett. **85**, 2895 (2000).
- [22] M. G. Bowler, Phys. Lett. **B270**, 69 (1991).
- [23] Y. M. Sinyukov, R. Lednicky, S. V. Akkelln, J. Pluta and B. Erasmus, Phys. Lett. **B432**, 248 (1998).
- [24] D. Adamová *et al.* (CERES Collaboration), Nucl. Phys. **A714**, 124 (2003).
- [25] S. S. Adler *et al.* (PHENIX Collaboration), Phys. Rev. Lett. **93**, 152302 (2004).
- [26] K. Morita, S. Muroya and H. Nakamura, in preparation.